MOLECULAR AND CELLULAR BIOLOGY, Nov. 2011, p. 4582–4592 Vol. 31, No. 22
0270-7306/11/$12.00 doi:10.1128/MCB.05730-11

The *Drosophila javelin* Gene Encodes a Novel Actin-Associated Protein Required for Actin Assembly in the Bristle[▽]

Shira Shapira, Anna Bakhrat, Amir Bitan, and Uri Abdu*

Department of Life Sciences and National Institute for Biotechnology in the Negev, Ben-Gurion University, Beer-Sheva 84105, Israel

Received 1 June 2011/Returned for modification 23 June 2011/Accepted 7 September 2011

The *Drosophila melanogaster* bristle is a highly polarized cell that builds specialized cytoskeletal structures. Whereas actin is required for increasing bristle length, microtubules are essential for bristle axial growth. To identify new proteins involved in cytoskeleton organization during bristle development, we focused on identifying and characterizing the *javelin* (*jv*) locus. We found that in a *jv* mutant, the bristle tip is swollen and abnormal organization of bristle grooves is seen over the entire bristle. Using confocal and electron microscopy, we found that in *jv* mutant bristles, actin bundles do not form properly due to a loss of actin filaments within the bundle. We show that *jv* is an allele of the predicted *CG32397* gene that encodes a protein with no homologs outside insects. Expression of the Jv protein fused to a green fluorescent protein (GFP) shows that the protein is colocalized with actin bundles in the bristle. Moreover, expression of Jv-GFP within the germ line led to the formation of ectopic actin bundles that surround the nucleus of nurse cells. Thus, we report that Jv is a novel actin-associated protein required for actin assembly during *Drosophila* bristle development.

Changes in cell shape, driven by cytoskeleton structures within the cell, are fundamental processes that allow cells and tissues to adopt new shapes and functions. The highly polarized shape of the *Drosophila melanogaster* mechanosensory bristle makes it a good model for studying the role of the cytoskeleton during cell elongation. Since the cytoskeleton plays a crucial role in the development of these highly polarized bristles, any changes in bristle organization would result in an easily detectable phenotype in adult flies (22). Bristles sprout from the subepidermal layer during metamorphosis, 32 h after puparium formation (APF), and elongate over the course of 16 h (24). Bristles can be divided into microchaetes and macrochaetes based on their size, number, and location. The 200 microchaete bristles, ordered in evenly spaced rows, have an average length of 70 μm. In contrast, the 22 macrochaetes on the fly's dorsal thorax can reach lengths of up to 400 μm each (11, 19).

Bristle growth is driven by actin filament polymerization (22), with actin filaments being continually formed at the bristle tip, where they are cross-bridged into modules. These modules are attached end to end into firm bundles that lie against the membrane. Bundle formation is achieved in a three-stage process by at least two cross-linking proteins, forked and fascin (19, 20, 23). Once elongation is complete, the actin bundles decompose (~53 h APF) and a thick layer of chitin supports the cell in place of the bundles (9, 20). Thus, at the end of this process, the bristle of the adult fly presents a grooved pattern. The valleys of the bristle represent regions where membrane-attached actin bundles were positioned, while the bristle ridges correspond to regions that lacked actin bundles (19).

In addition to actin bundles, a large population of microtubules (MTs) is also found in the bristle shaft. It was shown that the majority of the MT array, which is shorter than the length of a mature bristle, assembles early in development, although the mechanism by which the MT network is organized remains unknown (22). Since microtubule antagonists injected immediately prior to the time of bristle initiation led to the appearance of shorter and fatter bristles than seen in untreated flies (5), it was suggested that microtubules assume an important role in maintaining bristle axial growth. Moreover, it was demonstrated that during bristle elongation, treatment with microtubule antagonists had no effects on microtubule network density, suggesting that MTs within the bristle shaft are stable (22). Recently, we have shown that MTs are organized in a polarized manner, i.e., minus end out, and that this MT organization is require for the bristle axial shape (2).

javelin (*jv*) is a spontaneous mutation that was identified in 1947. *jv* mutant bristles do not taper like bristles in wild-type flies, instead presenting a small enlargement before the tip. It was shown that *jv* is cell autonomous and useful as a marker for epidermal clones (14). Since *jv* affects bristle development, we focused on the further characterization of *jv* phenotypes and the identification of the encoding gene. We have shown that in *jv* mutants, the bristle tip becomes swollen, resembling a spear (13), rather than assuming the pointed tip seen in wild-type bristles. We showed, furthermore, that *jv* mutant bristles display an irregular groove pattern with unparallel and shallower ridges. Now, closer examination of actin bundle arrangement in *jv* mutants using transmission electron microscopy (TEM) reveals that the loss of actin filaments within the bundles affects the triangular structure of the bundles. We also demonstrate that the *jv* mutant carries the predicted *CG32397* gene and that this gene encodes an actin-associated protein. Thus, our study identifies Jv as a novel actin-associated protein required for actin assembly.

* Corresponding author. Mailing address: Ben-Gurion University, Ben-Gurion Blvd., Beer-Sheva 84105, Israel. Phone: 972-8-6479072. Fax: 972-8-6461710. E-mail: abdu@bgu.ac.il.

▽ Published ahead of print on 19 September 2011.

MATERIALS AND METHODS

***Drosophila* stocks.** The following mutant and transgenic fly strains were used. The CG18769[c03230], CG18769[EY01803], jv^1, nd^{11}, nd^{14}, Zpg^{96}, Zpg^{107}, Df(3L)BSC410, Df(3L)Exel9058, Df(3L)BSC437, Df(3L)Exel7210, Df(3L)BSC411, Df(3L)Exel8101, Df(3L)ED211 Df(3L)Exel6109, Df(3L)BSC27, Df(3L)BSC224, and w[1118]; CyO, P{Tub-PBac\T}2/wg[Sp-1] lines were all obtained from the Bloomington Stock Center. Germ line and bristle expression was performed with P{matα4-GAL-VP16}V37 (referred to as α-*tub Gal4-3*) and *neur-Gal4*, respectively. Ubiquitous expression was performed with actin5C-Gal4. All of the Gal4 lines were obtained from the Bloomington Stock Center. The following upstream activation sequence (UAS)-RNA interference (RNAi) lines, designated by transformant identification number, were obtained from VDRC, Austria: *CG18769* RNAi, 9501; *CG32397* RNAi, 103870; *CG8368* RNAi, 108563; *CG8398* RNAi, 35927; and *CG8398* RNAi, 35928.

Developmental staging and pupa dissection. For examination of the bristles in wild-type and mutant flies, white prepupae were collected and placed on double-sided Scotch tape in a petri dish placed in a 25°C incubator as previously described (22). At the appropriate time of incubation (38 to 48 h), the pupae were dissected by removing the pupal case, and the pupae were filleted in phosphate-buffered saline (PBS), pH 7.35 to 7.45, as described previously (21). The thoracic fillet was then placed on its back, and the internal organs and fat bodies were removed (22). The clean tissue was fixed for light or electron microscopy.

Bristle phalloidin and antibody staining. Clean thoraces were fixed in 4% paraformaldehyde in PBS for 20 min and then in 4% paraformaldehyde containing 0.3% Triton X-100 in PBS for an additional 20 min. The samples were washed three times with 0.3% Triton X-100 in PBS for 10 min each time. For antibody staining, the thoraces were blocked in 0.1% Triton X-100 containing 4% bovine serum albumin and 0.1% NaN_3 for 1 h. The samples were then incubated with a primary antibody in the above-mentioned blocking solution overnight at 4°C, washed three times in 0.3% Triton X-100 in PBS, and incubated with secondary antibodies and phalloidin in blocking solution for 2 h at room temperature or at 4°C overnight in the dark. After such incubation, the samples were washed three times with 0.3% Triton X-100 in PBS for 10 min each time and then placed on a slide and mounted in Citifluor glycerol (Ted Pella, Redding, CA). A coverslip was placed on the sample, and the preparation was sealed with nail polish. The slides were examined with an Olympus FV1000 laser-scanning confocal microscope. The images are presented as *z*-axis projections of several optical sections that collectively cover the bristle diameter. Rabbit antiforked (1:100), mouse antifascin (1:100) (provided by G. M. Guild and K. Cant, respectively), mouse anti-spn-F (1:10) (1), and mouse anti-α-tubulin (1:250) (Sigma) primary antibodies were used. Goat anti-mouse Cy2 and Cy3 and goat anti-rabbit Cy3 (Jackson ImmunoResearch) secondary antibodies were used at a dilution of 1:100. The goat anti-rabbit Cy3 (Molecular Probes) secondary antibodies were used at a dilution of 1:500. For actin staining, we used Oregon Green 488- or Alexa Fluor 568-conjugated phalloidin (1:250) (Molecular Probes).

Real-time RT-PCR. Total RNA was extracted after removing the pupal cases from pupae 48 h after pupariation by using the NucleoSpin RNA II kit, including DNase treatment, according to the manufacturer's instructions (Macherey-Nagel). cDNA was transcribed from 1 to 5 μg total RNA using reverse transcriptase and oligo(dT) (ABgene) according to the manufacturer's instructions (Bio-Lab, Beit Haemek, Israel). Reverse-transcribed total RNA (100 ng) was amplified in a 20-μl reaction mixture containing 100 nM concentrations of each primer and 10 μl of SYBR green PCR master mix (Stratagene). Reverse transcription (RT)-PCR was performed to amplify CG32397 cDNA using primers CG32397 Fwd (5′-AACGTTGACTTGGCCTACAC-3′) and CG32397 Rev (5′-AACTTCGCGCAGTTGTTTTC-3′). To normalize differences in total cDNA between samples, cDNA from ribosomal protein 49 was amplified using primers Rp49 Fwd (5′-CCGCTTCAAGGGACAGTATCTG-3′) and Rp49 Rev (5′-CACGTTGTGCACCAGGAACTT-3′). PCR conditions were as follows: the reaction mixtures were first kept at 95°C for 15 min, then 40 cycles of PCR (95°C for 30 s, 55°C for 1 min, and 72°C for 1 min) were performed, and finally, the mixtures were incubated at 95°C for 1 min, 55°C for 30 s, and 95°C for 30 s. All quantitative PCR analyses were performed in triplicate. Real-time PCR was performed using the Mx3000p machine (Stratagene, La Jolla, CA), and the amount of gene product in each sample was determined by the comparative quantification method using MxPro software (Stratagene).

Genomic organization of *CG32397* and 5′ RACE. To amplify the gene *CG32397* from cDNA prepared from pupae 48 h APF, we used several primer sets that cover the entire region of the gene. The first forward primer designed from the predicted start codon, FW1 (5′-ATGACAAGCCGCAGTTTTATTATC-3′), was unable to amplify a product together with the reverse primer, REV1 (5′-GGATGCAATTGCTCACTCAG-3′). Thus, we performed 5′ rapid amplification of cDNA ends (RACE) as described below to identify the 5′ end of the gene. For this, we used a forward primer corresponding to the new predicted translation start site, FW1 New (5′-ATGGGCAACGGATATTTTCG-3′). The rest of the sequence was amplified using primer pairs FW2 (5′-CAGCAGCAACATCAACAGCA-3′) and REV2 (5′-CCACTACAGCTAGGATATTC-3′), FW3 (5′-TCCTCTGTTAACCACCACAG-3′) and REV3 (5′-CTGAACGAGATTACAAGTTG-3′), FW4 (5′-AGAAGGAGGCAATTCAGGAG-3′) and REV4 (5′-GAACAGTCGTAGGCGTAGTTG-3′), FW5 (5′-CAACAATAATGTGGTGATAG-3′) and REV5 (5′-ACACATTGCAGGCCTCGATTTG-3′), and FW6 (5′-TACTACGGAGGAAGAGTGCTG-3′) and REV6 (5′-CATTTGTCATCCAGGC-3′).

To identify the 5′ end of the *CG32397* gene, single-stranded cDNA was reverse transcribed from 1 to 3 μg RNA extracted from wild-type pupae using BD PowerScript reverse transcriptase, 5′-CDS primer, and BD Smart II A oligo (BD Smart RACE cDNA amplification) according to the manufacturer's instructions (Clontech). 5′ RACE was performed using a gene-specific primer (5′-CGAAAATATCCGTTGCCCATCGTG-3′) and a universal primer from the kit. The PCR conditions used were as follows. There were five initial PCR cycles consisting of 94°C for 30 s and 72°C for 3 min. Five additional cycles of 94°C for 30 s, 70°C for 30 s, and 72°C for 3 min followed. Finally, 25 PCR cycles consisting of 94°C for 30 s, 68°C for 30 s, and 72°C for 3 min were conducted. The RACE product was analyzed by 1% agarose gel electrophoresis, and the fragment was purified using a DNA isolation kit (Biological Industries), subcloned into the pGEM-T vector (Promega), and sequenced.

SEM. Adult *Drosophila* flies were fixed and dehydrated by immersion in increasing concentrations of ethanol (25%, 50%, 75%, and twice in 100%; 10 min each). The flies were then completely dehydrated using increasing concentrations of hexamethyldisilazane (HMDS) in ethanol (50%, 75%, and twice in 100%; 2 h each). The samples were air dried overnight, placed on stubs, and coated with gold. The specimens were examined with a scanning electron microscope (SEM; JEOL model JSM-5610LV). Length measurements of adult bristles were performed using Image J (version 1.40j) software.

TEM. At 42 h APF, the dorsal surface of the thorax of each pupa was dissected as described above and fixed for 20 min in 2% glutaraldehyde in 0.2 M PO_4 (pH 6.8) at room temperature and then for 1 h on ice. After 1 h, the specimens were transferred to a fixative comprising cold water, 0.2 M PO_4 (pH 6.2), 4% osmium tetroxide (OsO_4), and 50% glutaraldehyde and placed on ice for 1 h. The specimens were then washed three times in cold water (20 min each) and incubated in 1% uranyl acetate overnight at 4°C. This was followed by transfer to a dehydration series spanning from 30 to 100% acetone, with 10% increases being made at each 15-min interval. Samples were then treated twice in propylene oxide for 15 min and soaked for 1 h in a 1:1 solution of propylene oxide and araldite, followed by overnight incubation at 4°C in a 1:2 propylene oxide/araldite mixture. The tissues were then transferred to araldite and incubated for 1 h, placed on araldite blocks (the blocks were polymerized a day before at 60°C), and embedded in araldite. These were then left at room temperature for 30 min after embedding, at which point the samples were oriented and incubated at 60°C for 24 h. Transverse sections were cut through the thorax using a Leica UltraCut UCT ultramicrotome equipped with a diamond knife, stained with uranyl acetate and lead citrate, and then examined with a JEOL JEM-1230 transmission electron microscope operating at 120 kV.

Transgenic flies. To clone gene *CG32397* in the pUASp vector containing DNA encoding green fluorescent protein (GFP), total RNA was extracted from wild-type pupae 48 h APF using a NucleoSpin RNA II kit and cDNA was transcribed according to the manufacturer's instructions (Bio-Lab). Cloning of the entire open reading frame was achieved in two steps, as follows. In the first step, the last 3,147 nucleotides of the 3′ end of the gene were PCR amplified and introduced into the XbaI site of pUASp-GFP as an XbaI-SpeI fragment. In the second step, the first 2,538 nucleotides were added as an XbaI-XbaI fragment. To generate transgenic flies, a P-element-mediated germ line transformation of this construct was carried out according to standard protocols (18).

Yeast two-hybrid assay. A yeast two-hybrid analysis was performed using the yeast two-hybrid Phagemid vector kit (Stratagene) according to the manufacturer's instructions. The pAD-CG32397 plasmid was used as bait, while plasmids encoding actin were used as prey. The YRG2 host strain (Stratagene) was cotransformed with plasmid pAD-CG32397 and with pBD-actin plasmids using the lithium acetate (LiAc) method. Positive interactions were tested by selection on plates with synthetic dextrose medium lacking histidine (SD−His).

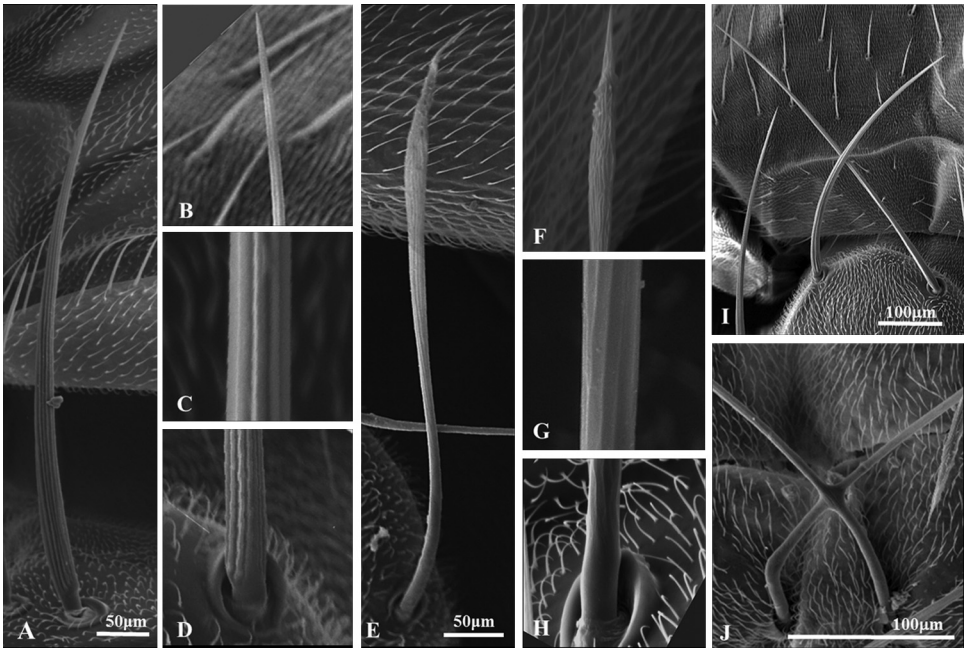

FIG. 1. Mutations in *jv* affect bristle development. Scanning electron micrographs of wild-type (A to D) and jv^1 mutant (E to H) bristles are shown. The ridges in the middle and lower parts of the jv^1 bristle (G and H) are disorganized. They are shallower and thinner than wild-type bristles (C and D). The jv^1 bristle tips (F) are swollen and contain misaligned, smaller ridges than seen in the wild-type bristle tips (B). In addition, some of the mutants present fused posterior scutellar bristles (J) that do not separate from one another, unlike in the wild type (I).

RESULTS

Analysis of the bristle defects in the *javelin* mutant. Since bristle morphology reflects the organization of the cytoskeleton in the bristle (6, 8), we examined the external cuticular structure of macrochaetes by SEM. While the wild-type bristle surface presented pronounced, straight ridges and valleys (Fig. 1A to D), the mutants' bristles appeared in a smoother cuticular pattern in which the ridges were shallower and thinner than in the wild-type bristles (Fig. 1E to H). In addition, instead of tapering toward the tip (Fig. 1B), the mutants' bristles become bulbous at the tip, giving the bristle the shape of a spear (Fig. 1F). Furthermore, the bristle tip has abnormally organized surface grooves, with the ridges not being parallel to each other (Fig. 1F). In addition to these irregular groove patterns, we also found that in 25% of the flies, the posterior scutellar bristles are fused (Table 1 and Fig. 1J). In both wild-type and *jv* mutants, these bristles grow diagonally and cross each other (Fig. 1I); however, in the *jv* mutants, it seems that these bristles fused together at their meeting points.

Since variations in bristle length can indicate changes in the cytoskeleton (5, 22), we measured the lengths of the anterior and posterior scutellar macrochaetes. We found no significant difference between these lengths in the wild-type and mutant bristles (Table 1).

Actin bundles are disorganized in *jv* mutant bristles. Since *jv* mutant bristles exhibit an aberrant morphology that appears to be cytoskeleton related, we analyzed actin cytoskeleton organization during pupal development. Initially, we examined the bristles 42 h APF using confocal microscopy. Phalloidin staining of actin bundles revealed that while wild-type bristles taper in a straight direction toward the tip (Fig. 2A and B), *jv* mutant bristles remain wide (Fig. 2C and D). Next, we examined the bristles 48 h APF, when the bristles are fully elongated. During this developmental stage, the defective spatial

TABLE 1. Summary of bristle phenotypes from *jv* mutant and rescue flies[a]

Phenotype or parameter	Value for genotype[b]					
	Wild type	jv^1	jv^1/jv^2	*Actin-Gal4;* pUAS-*CG32397* RNAi	*Actin-Gal4*; jv^1-pUAS-GFP-*CG32397*	*Actin-Gal4*: jv^1-pUAS-GFP-*CG32397*/jv^2
Fused bristle	0 (0/324)	25.8 (37/143)	14.9 (10/67)	13.3 (6/45)	2.9 (2/68)	2.3 (1/42)
Avg length of macrochaetes[c]	313.6 ± 44.7 (23)	308.5 ± 58.1 (27)	312 ± 34.2 (12)	310 ± 55.3 (15)	309 ± 47 (12)	314 ± 39 (16)
Bulbous tip	0 (0/145)	62.5 (60/96)	53.9 (41/76)	56.6 (30/53)	30.6 (30/98)	34.9 (22/63)

[a] All of the results presented in the table were taken from females. Similar results were also noted for males.
[b] Values for fused bristle and bulbous tip phenotypes are percentages (number of flies with the genotype/total number of flies). Average lengths of macrochaetes and standard deviations are in micrometers (number of macrochaetes measured).
[c] Average length of anterior scutellar macrochaetes. Similar results were also found for posterior scutellar macrochaetes.

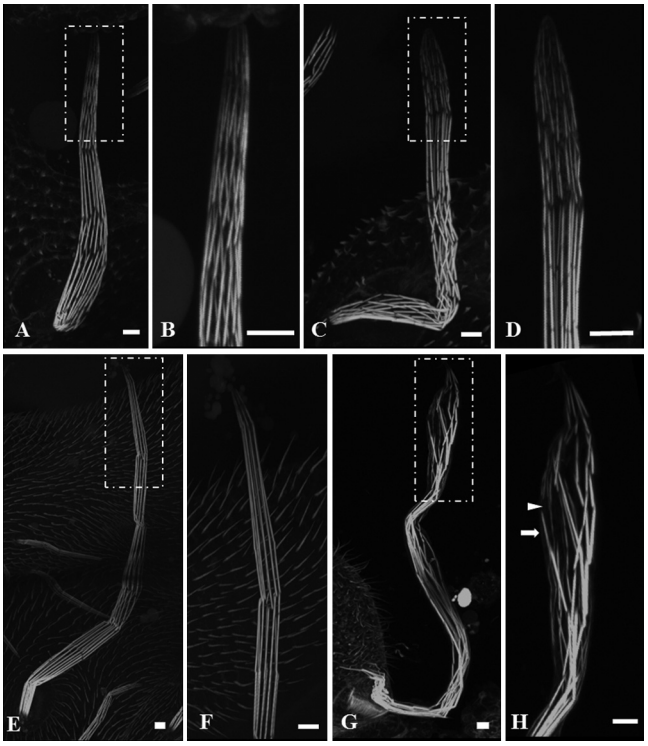

FIG. 2. Disorganization of actin bundles in the *jv* mutant. Confocal microscopy projections of macrochaetes from 42-h-old (A and B) and 48-h-old (E and F) wild-type pupae and from 42-h-old (C and D) and 48-h-old (G and H) *jv* pupae. Actin bundles are stained with Oregon Green-phalloidin (gray). The bristle tip of a 42-h-old *jv* pupa (C; the area shown in the white rectangle is enlarged in panel D) is not tapered, as it is in the wild type (A and enlargement in panel B). At 48 h APF in the *jv* mutant, the actin bundles along the entire bristle run in different directions (G). The bristle tip (enlargement in panel H) is swollen, and the actin bundles in this region are not parallel to each other, as they are in the wild type (enlargement in panel F). Moreover, some of the bundles are thinner (enlargement in panel H, arrowhead) than others (enlargement in panel H, arrow). Scale bars, 5 μm.

organization of actin bundles is more pronounced than in bristles 42 h APF. At the later time point, the bundles are disordered and run in different directions along the bristle shaft and some appear to be thinner than others (Fig. 2G). These actin bundle defects seem to be more severe at the swollen bristle tip (Fig. 2H), giving the bristle a spear-like shape.

To visualize the internal organization of actin bundles, we examined thin transverse sections of bristles 42 h APF by electron microscopy. While the actin membrane-associated bundles have a triangular shape in wild-type bristles (Fig. 3A to A″), in *jv* mutant bristles, the actin bundles were no longer triangular in shape (Fig. 3B', B″, C', and C″). It is of note that in most cases, there were gaps in some of the bundles where no actin filaments could be found (Fig. 3B' and C'). In some extreme cases, the bundles in the mutants were larger than those of the wild type due to the more disordered arrangement of the filaments (Fig. 3C to C″). Groups of filaments tend to aggregate together, thus creating gaps or spaces within the bundle, giving a perforated appearance. In addition, the actin filaments are not fully attached to the plasma membrane, which causes the poorly organized bundles to be less associated with the membrane (Fig. 3C' and C″).

Localization of the actin cross-linking proteins, forked and fascin, is not affected in *jv* mutant bristles. *Drosophila* bristles sprout 32 h APF during metamorphosis and elongate over the course of 16 h (24). This elongation is driven by actin bundles (22). Thus far, two known cross-linking proteins have been discovered, forked and singed (a fascin homolog), which are involved in actin construction in *Drosophila* bristles (20). Since actin filaments in *jv* mutant bristles do not gather properly into compact, maximally cross-linked bundles, we performed antibody staining of *Drosophila* fascin and forked proteins. Immunofluorescent staining of developing mutant bristles in forked proteins (Fig. 4E) revealed the localization of the protein to be similar to that of wild-type bristles (Fig. 4B). In both wild-type and *jv* mutant bristles, forked is present along the entire length of the actin bundles and is also concentrated in the gaps between the actin bundles (7) (Fig. 4 A to F). Fascin protein was evenly diffused in the cytoplasm and in the socket cell of the bristle in wild-type flies (4) (Fig. 4G). A similar distribution was seen in the *jv* bristle (Fig. 4H).

The MT array in *jv* mutants is normal. In addition to actin bundles, there is a large population of MTs, which run longitudinally along the bristle shaft (2, 22). Like actin, these MTs play an important role as cytoskeleton components in *Drosophila* bristles (22). Since inhibitor-based (5) and genetic (2) studies showed that disorganization of MTs can also lead to morphological defects of the bristles, we investigated the organization of MTs in *jv* mutant bristles. Specifically, we examined how MTs are arranged in the mutant by immunostaining developing bristles with anti-α-tubulin antibodies. Examination of the *jv* mutant bristles revealed that the microtubule array is properly organized (Fig. 5E), as in wild-type bristles (Fig. 5B).

Next, we checked whether MT functionality is affected in the *jv* mutants. The MT network serves as a transport system for different proteins in bristles (2). Previous studies showed that those several proteins (among them, spn-F and hook) are localized asymmetrically within the bristle shaft, where they accumulate at the bristle tip (2, 17). When the MT array is disorganized, spn-F and hook proteins do not reach their natural positions but rather accumulate along the bristle shaft (2). Therefore, we used spn-F and hook proteins as markers to inspect the polar transport system in the mutant bristles. Staining of wild-type bristles with anti-spn-F antibodies 42 h APF showed that the protein is localized at the bristle tip (2) (Fig. 5G). A localization pattern for spn-F was found to be similar to that in the *jv* mutant bristle (Fig. 5H). Similar results were also found for the hook protein (data not shown).

Molecular characterization of the *javelin* locus. The *jv* mutation was identified in 1947 and mapped to region 65A1-65E1 (Flybase [http://flybase.org/]). However, the gene affected by this mutation was not defined. Using deficiency mapping, we showed that the *jv* gene is found in region 65B4-65C1, which includes 7 different genes. To identify the sequence corresponding to the gene encoding Jv, we took two approaches. In the first, we tested whether *jv* mutants fail to complement known mutations in this region, namely, in the *ndl* and *zpg* genes. In the second approach, we performed RNAi silencing of the other genes in the bristle using inducible RNAi in

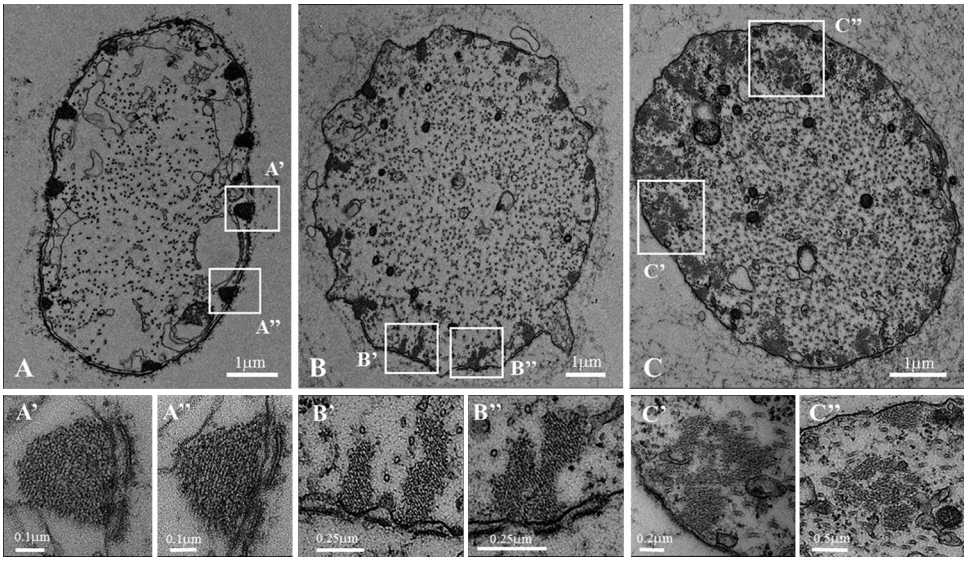

FIG. 3. Defects in the internal organization of actin bundles in a *jv* mutant. Thin transverse sections of microchaete bristles from 42-h-old wild-type pupae (A, A', and A″) and 42-h-old *jv* pupae (B to B″ and C to C″). In wild-type bristles, actin bundles are composed of a hexagonally packed array of actin filaments and assume a triangular shape (higher magnification in panels A' and A″). The bundles in *jv* mutants are not organized properly and lack the triangular shape (B and C). The filaments are not tightly packed, thus creating gaps within the bundle (B' and B″). In extreme cases, the bundles are larger than those in the wild type and have more space between groups of filaments (C'). Also, these bundles are not fully attached to the plasma membrane (C' and C″). Scale bar sizes are indicated.

a Gal4/UAS system (3, 15). We found that downregulation of one novel gene, *CG32397*, affected bristle morphology (Fig. 6D). When this gene was affected, the bristle ridges were shallow, as in *jv* mutants (Fig. 6B), and toward the bristle tip, the ridges became disorganized and nonparallel to one another. In addition, there was a spear-like shape to the bristle. We also found that in 13.3% of the flies, the posterior scutellar bristles were fused (Table 1).

To verify that *CG32397* encodes Jv, we sequenced the *CG32397* coding region from genomic DNA of the jv^1 mutant stock and compared the sequence obtained to that of the wild type. No mutations were found in the coding region of the *CG32397* gene in the jv^1 mutant.

Next, we performed real-time PCR to verify that our RNAi silencing indeed reduced the levels of the *CG32397* transcript.

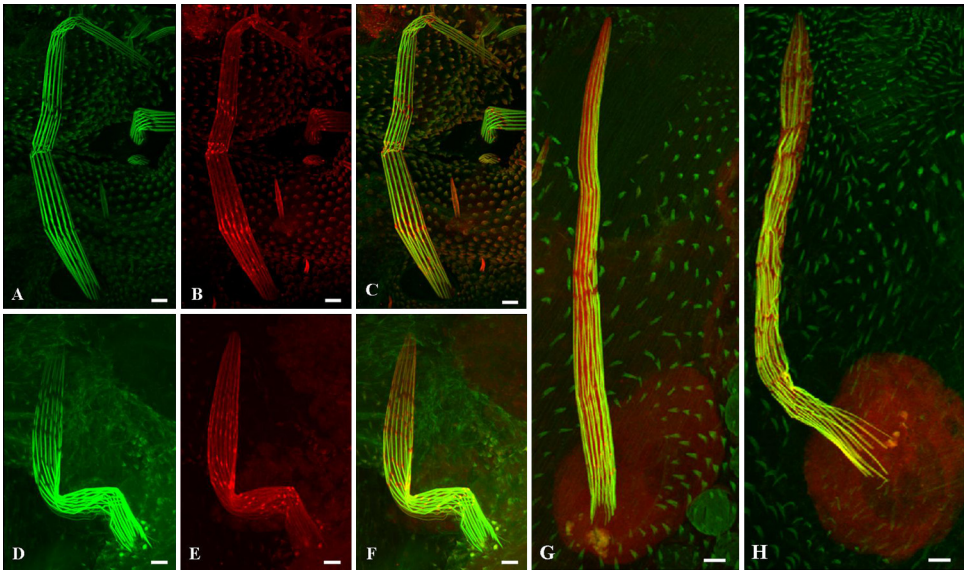

FIG. 4. Actin cross-linkers are properly localized in the *jv* mutant. (A to F) Confocal microscopy projections of bristles from 42-h-old wild-type pupae (A to C) and 42-h-old *jv* pupae (D to F) stained with antiforked antibodies (red). (G and H) Confocal microscopy projections of bristles from 42-h-old wild-type pupae (G) and 42-h-old *jv* pupae (H) stained with antifascin antibodies (red). The actin bundles in the bristles were stained with Oregon Green-phalloidin (green). In *jv* mutants (E and F), as in wild-type bristles (B and C), the forked protein is localized along the actin bundles and in the gaps between them. The fascin protein was evenly diffused in the cytoplasm and in the socket cell of the bristle in both *jv* mutant (H) and wild-type (G) bristles. Scale bars, 5 μm.

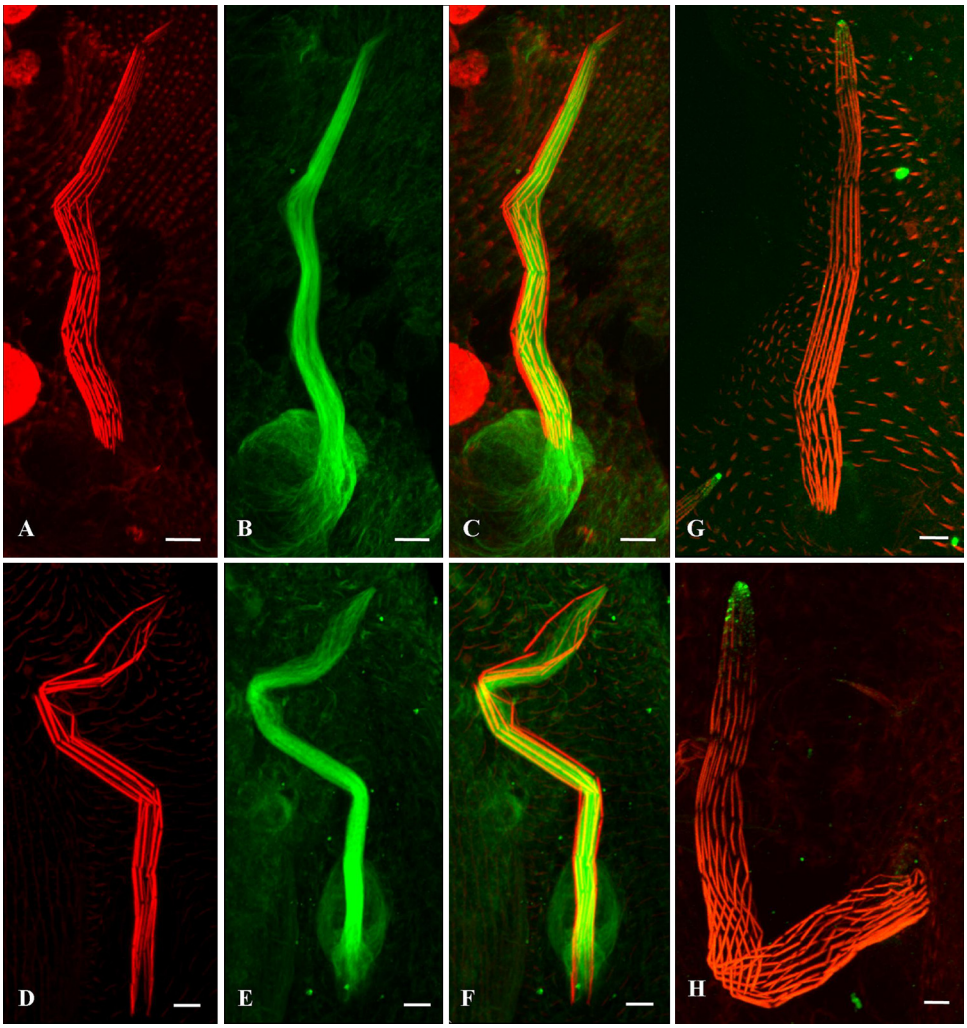

FIG. 5. Mutations in *jv* do not affect microtubule network organization. (A to F) Confocal microscopy projections of bristles from 45-h-old wild-type pupae (A to C) and 45-h-old *jv* pupae (D to F) stained with anti-α-tubulin antibodies (green) and Alexa Fluor-phalloidin (red). *jv* mutants exhibit a microtubule array along the bristles that is properly organized (E), as in wild-type bristles (B). (G and H) Confocal microscopy images of bristles from 42-h-old pupae (G and H) stained with anti-spn-F antibodies (green) and Alexa Fluor-phalloidin (red). In both *jv* mutant (H) and wild-type (G) bristles, spn-F is localized to the bristle tip. Scale bars, 5 μm.

We calculated the relative change (12) in *CG32397* gene expression after RNAi silencing and found that the transcript level decreased almost 3.3-fold compared to that of the control. Next, we searched for several alleles of the *CG32397* gene and found 11 known transposon insertions in the gene area. Only two of these are available from the Bloomington collection (CG18769[c03230] and CG18769[EY01803]). We found that only homozygous CG18769[c03230] flies showed defects in bristle development which resemble the jv^1 bristle phenotype (data not shown). Moreover, we found that jv^1 fails to complement the bristle phenotype when crossed to flies bearing the P element (Fig. 6E). Next, we tested whether excision of the piggyBac element (CG18769[c03230]) from the *CG32397* gene could revert the bristle phenotype to a wild-type-like phenotype. As expected, excision of the P element reverted the bristle phenotype to that of the wild type. Moreover, after P element excision, this fly line complemented the jv^1 bristle phenotype (data not shown). For clarity, we will subsequently refer to the spontaneous mutation in the original mutant stock of *jv* as jv^1, while the CG18769[c03230] line will be referred as jv^2. Next, we performed real-time PCR to analyze the transcript levels of *CG32397* in jv^1 and in jv^2 and found that the transcript levels of *CG32397* decreased 4.9-fold in jv^1 and 1.5-fold in jv^2 compared to those of wild-type flies.

Since *CG32397* is a predicted gene lacking molecular data, we decided to verify the predicted open reading frame of this gene. To this end, we designed several primer sets that cover the entire predicted region of the gene (Fig. 7A). Using these sets of primers (see Materials and Methods), we were able to amplify almost the entire gene from cDNA prepared from pupae 48 h APF. However, we were unable to amplify the 5′ end of the predicted gene. Thus, we performed 5′ RACE to reveal the organization of this predicted gene. We found a discrepancy between the predicted gene and the 5′ RACE result. We saw that the first translation start site is located 165 bp downstream of the predicted N-terminal methionine (Fig.

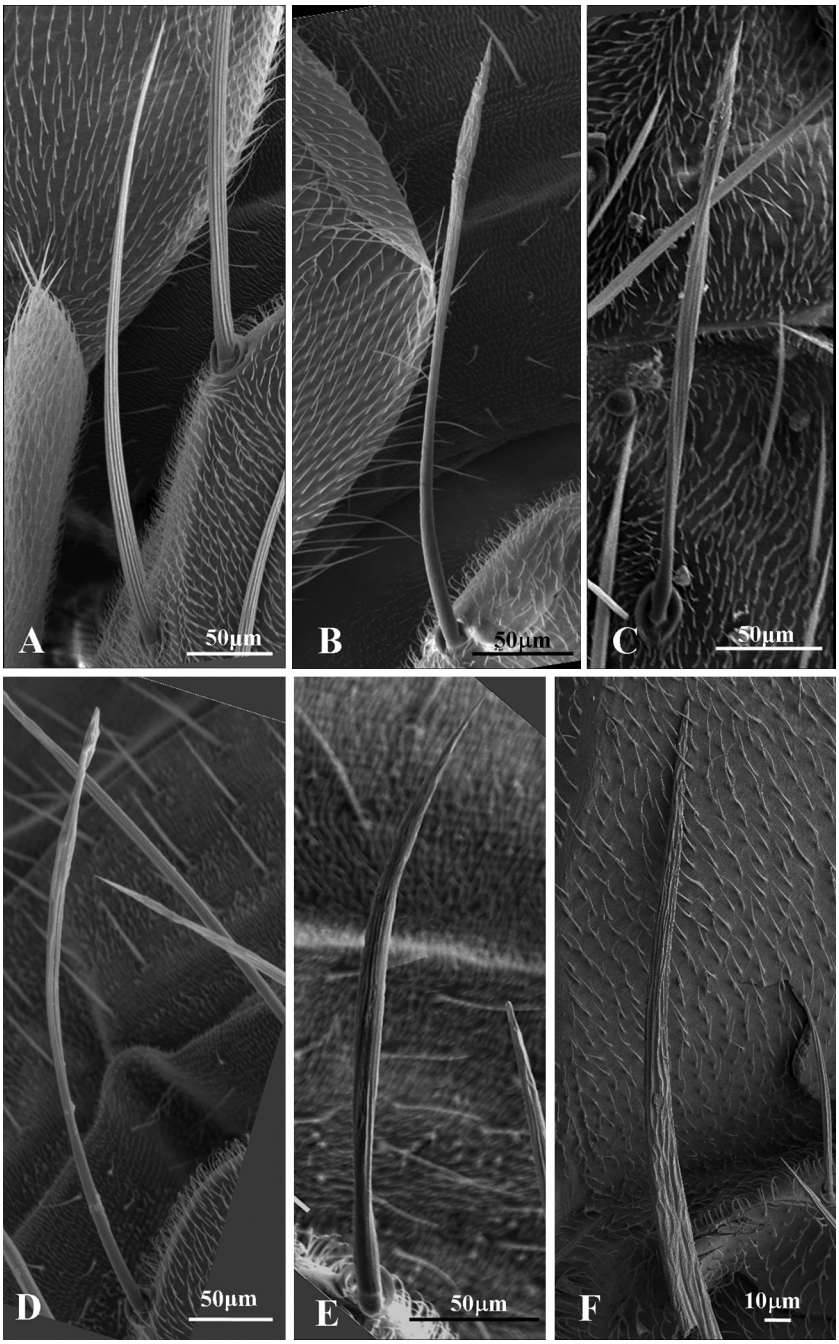

FIG. 6. Jv is encoded by the *CG32397* gene. Scanning electron micrographs represent bristles of wild-type (A), jv^1 mutant (B), jv^1 hemizygous (C), *Act-Gal4*; pUAS-*CG32397* RNAi (D), jv^1/CG18769[c03230] (E), and *actin-Gal4-*jv^1; pUAS-GFP-*CG32397* (F) flies. RNAi silencing of *CG32397* in the bristles (D) has the same phenotype as in jv^1 mutant bristles (B). (E) CG18769[c03230] fails to complement jv^1 bristle defects. (F) GFP-CG32397 rescues the jv^1 bristle phenotype. Although the ridges are disorganized, they are more pronounced than in jv^1 mutant bristles. Moreover, the bristle tapers toward the tip and it is not swollen, as it is in jv^1 mutants (B). Scale bar sizes are indicated.

7B and C) and that the open reading frame was unchanged but predicted a product reduced by 55 amino acids. Moreover, we were able to show that the 5′ untranslated region (UTR) is expanded into 3 exons, the first containing 78 bp and located 1.7 kbp from the second exon, the second located 3.8 kbp from the new translation start site and containing 207 bp, and the third containing 130 bp directly upstream of the first methionine (Fig. 7B and C). Thus, our results reveal a new organization of *CG32397* at the 5′ end of the gene. More importantly, our findings predict a gene product shortened from the previously predicted gene product by 55 amino acids at the N terminus.

Next, we performed rescue experiments by expressing the CG32397 protein in the jv^1 or jv^1/jv^2 mutant background. We

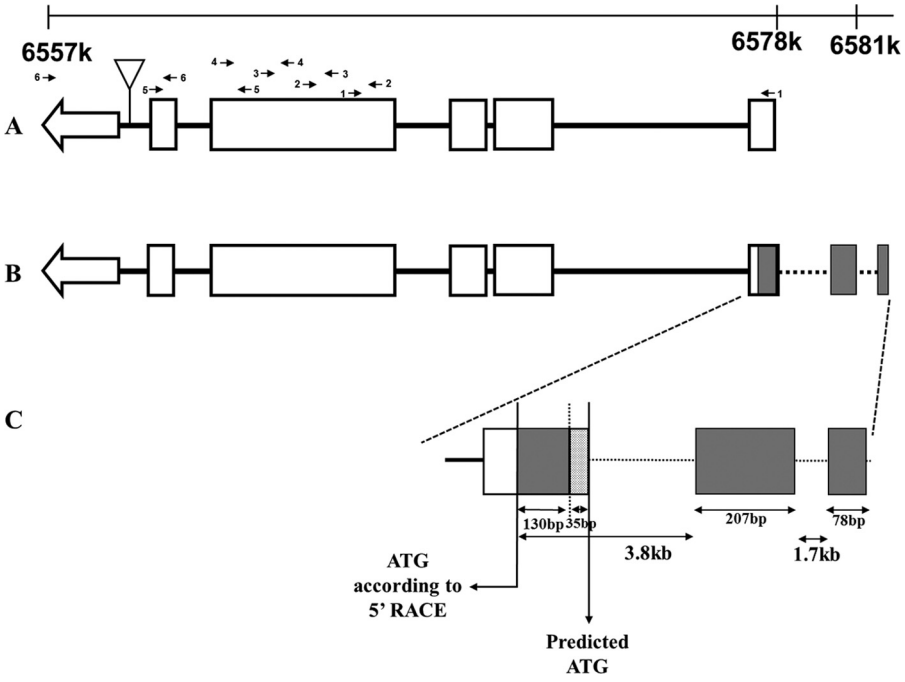

FIG. 7. Genomic organization of the *CG32397* gene. (A) A schematic diagram of the predicted sequence of *CG32397*. The white rectangles represent exons, while the black lines represent the introns of the gene. The small black arrows represent the six pairs of primers that were used to amplify *CG32397* from cDNA. The first primer pair failed to amplify the gene. The triangle between the fifth and sixth exons represents a transposon insertion (CG18769[c03230]) that failed to complement jv^1 bristle defects. (B) A schematic diagram of the sequence of *CG32397* according to 5′ RACE. The gray rectangles represent the 3 exons in the 5′ UTR of the gene that were revealed by 5′ RACE. An enlargement of this area (C) shows that there is a disparity between the predicted sequence and the 5′ RACE result. The first 35 bp, represented by a stippled rectangle, do not exist in the sequence of the gene. Therefore, the first translation start site is located 165 bp downstream from the predicted methionine.

created transgenic flies expressing nontagged and GFP-fused CG32397 proteins (using the new, experimentally validated protein open reading frame) under the control of the UAS/Gal4 system. We addressed the ability of these flies to rescue the jv^1 or jv^1/jv^2 bristle phenotype. We found that whereas 62% of the bristles from jv^1 mutant flies (Fig. 6B) and about 54% of the bristles from jv^1/jv^2 flies had swollen tips (Fig. 6E, Table 1), only 30.6% of flies expressing CG32397 in the jv^1 mutant background had swollen tips (Table 1 and Fig. 6F), and in jv^1/jv^2, the percentage of flies having a swollen tip decreased to about 35% (Table 1 and data not shown). Moreover, we found that in 25% of jv^1 flies and about 15% of jv^1/jv^2 flies, the posterior scutellar bristles are fused (Table 1). Expression of CG32397 reduces the level of these fusion events to 3% in jv^1 and to 2.3% in jv^1/jv^2 flies. We noticed that in 95% of bristles from flies expressing CG32397 in *jv* mutant backgrounds, the ridges on the entire bristle length were not parallel to each other as they are in the wild type (Fig. 6F).

Jv protein is associated with actin filaments. The *CG32397* gene encodes a protein with no homologs outside insects. Bioinformatics analysis revealed that the protein does not contain any known domain. We noted that expression of GFP-fused CG32397 rescues the jv^1 bristle phenotype and hence decided to analyze the localization pattern of this GFP-fused protein in the bristle. We found that GFP-Jv (Fig. 8A) is localized along the actin bundles (Fig. 8B), as revealed by its colocalization with the actin-interacting dye phalloidin (Fig. 8C).

Next, we studied the effect of expression of GFP-Jv in ovaries. For this, we expressed the GFP-fused protein in the germ line using an α-*tub Gal4-3* driver. We saw that in nurse cells, expression of GFP-Jv led to the formation of an ectopic actin network that surrounded the nurse cell nucleus (Fig. 8E and F, insets). This nurse cell nucleus-associated actin network is not normally found in wild-type cells (Fig. 8D). Moreover, at later egg chamber developmental stages (stage 14) in some of the nurse cells, GFP-Jv was also found in the actin network that surrounds the nurse cell nucleus (Fig. 8G to I, insets). Thus, our results demonstrate that the Jv protein is associated with the actin network. Yet, the ectopic actin network that surrounds the nurse cell nucleus had no effect on female fertility or embryo development.

Next, we analyzed whether CG32397 physically interacts with actin monomers using a yeast two-hybrid assay. We found that CG32397 failed to interact with actin, suggesting either that CG32397 binds F-actin or that association of CG32397 with actin is mediated by other proteins.

DISCUSSION

Mutation in *jv* affects actin assembly in the bristle. To identify new players required for cytoskeleton organization during *Drosophila* bristle development, we focused on the identification and characterization of the *jv* locus. Our results demonstrate that *jv* is involved in the assembly of actin bundles during bristle development, as *jv* mutant flies display numerous de-

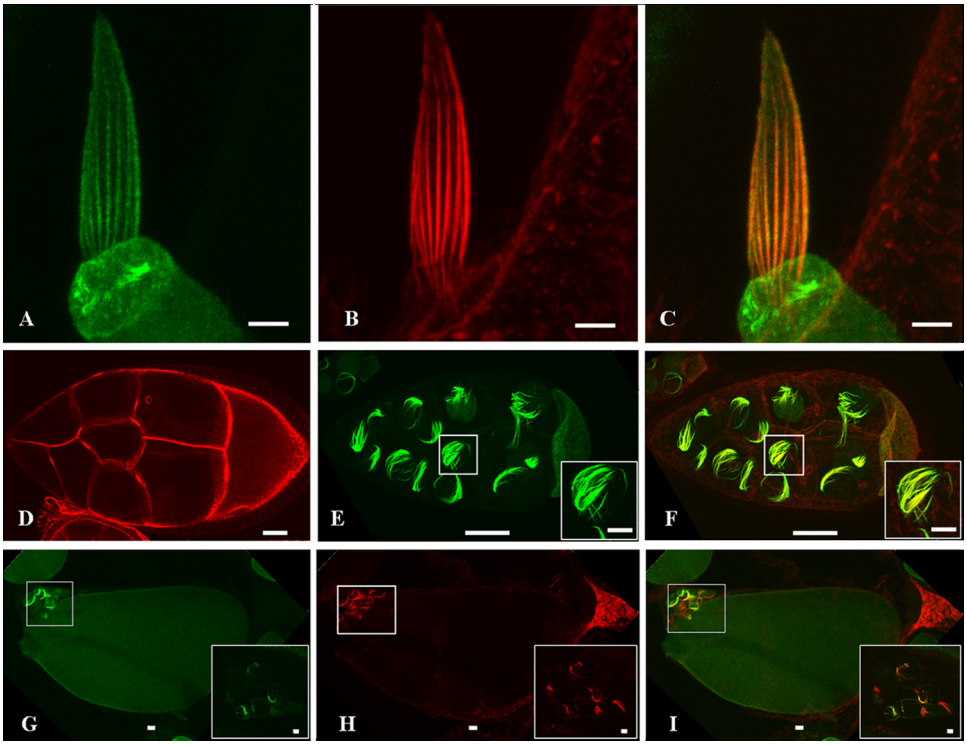

FIG. 8. GFP-Jv is colocalized with the actin bundles in the bristle and forms an ectopic actin network in the nurse cell nucleus. (A to C) Confocal microscopy projections of a 38-h-old pupa bristle from a *neur-Gal4*; pUAS-GFP-Jv transgenic fly (A, green) stained with Alexa Fluor-phalloidin (B, red) are shown. Panel C is a merger of panels A and B, showing that GFP-Jv is localized along the actin bundles. Scale bars for panels A to C, 5 μm. (E to I) Confocal microscopy projections of an ovary from an α-*tub Gal4-3*; pUAS-GFP-Jv transgenic fly at stage 8 (E and F, insets) and stage 14 (G to I). Both are stained with Alexa Fluor-phalloidin (red). In the nurse cells, GFP-Jv led to the formation of an ectopic actin network, surrounding the nucleus (E and F; see enlargements of this region), which is not found in wild-type cells (D). In stage 14, GFP-Jv is also colocalized with the actin that surrounds the nurse cell nucleus (G to I; insets are single-slice magnifications of this region). Scale bars for panels D to I, 30 μm (10 μm for the insets within each panel).

fects in bristle morphology. In the mutants, the lower part of the bristle is characterized by a smooth, grooved pattern, with the abnormality appearing more severe at the bristle tip. While in wild-type flies, the bristle is widest at the base and tapers toward the tip, in *jv* mutants, the bristle tip becomes bulbous, creating a spear-like shape. In addition, bristle ridges and valleys in this area are highly disordered and seem discontinuous. Since abnormalities in bristle morphology can indicate defects in the organization of the cytoskeleton within the bristle shaft, we examined the organization and functionality of bristle actin bundles and the microtubule array. We found that both the function and organization of the MTs are not affected in *jv* mutants. However, using confocal microscopy and actin staining, we revealed that the spatial organization of the actin bundles in the bristles is affected in *jv* mutants. Nonparallel actin bundles, some of which appeared to be thinner than others, were observed along the bristle shaft and especially at the bristle tip. These results led us to examine the internal organization of actin bundles in *jv* mutant bristles using TEM. Transverse sections through jv^1 bristles revealed defects in actin bundle formation. We noticed that the actin bundle no longer had the normal shape of a triangle that it had in a wild-type bristle. Instead, the actin bundles were disordered and presented gaps within them, leading to a perforated appearance. In some cases, we found that the actin bundles were not fully attached to the plasma membrane. It is important to mention that whereas confocal and SEM analysis was performed on macrochaetes, the TEM analysis was conducted on microchaetes. The reason for this was that defects in macrochaetes are easy to detect in the confocal microscope, while microchaetes are easy to analyze by TEM due to the fact that they are centrally positioned on the fly thorax and are more numerous than the macrochaetes. Therefore, the probability of getting thin transverse sections through the microchaetes is high (22).

How do the defects in the organization of the actin filaments in the bundles lead to aberrant bristle morphology in *jv* mutants? During bristle development, the cytoplasm projects between adjacent bundles, causing membrane protrusions. This creates the ridges seen in the adult bristle (20). In the areas where actin bundles are attached to the membrane, such protrusions cannot be accomplished, and as such, these regions will become the valleys seen in the cuticle (9, 20). Thus, while the cytoplasm projects through the interspaces between actin bundles in wild-type bristles, in *jv* mutants, the cytoplasm also projects within the bundles, forming protrusions in the membrane in areas where they are not supposed to be created. As a result, the ridges that form are highly disordered and shallower and appear to be noncontinuous along the bristle. Thus, we suggest that the loss of actin filaments within the bundle in

the *jv* mutant affects both actin bundle shape and bundle attachment to the membrane, which in turn affects bristle shape and morphology.

Another phenotype that we observed was fusion between the posterior scutellar bristles. At their meeting points, these *jv* mutant bristles have a shallower grooved pattern and a higher number of contact points between them than do wild-type bristles. Similar results were observed in response to the genetic interaction between *capping protein* β (*cpb*) and *arpc1* (6). Bristles from these mutant flies are also characterized by an irregular organization of ridges and valleys at the cuticle, as seen in *jv* mutants. Several processes could lead to bristle fusion, including secretion of chitin, as suggested by Frank et al. (6), or membrane fusion.

Jv is encoded by *CG32397*. In this study, we show that *jv* corresponds to the predicted gene termed *CG32397*. Several lines of evidence support our claim. (i) Using fine deficiency mapping of *jv* mutants, we showed that *jv* is found in the *CG32397* region. (ii) We showed that downregulation of the *CG32397* gene led to defects in bristle morphology, similar to the defects seen in *jv* mutants. (iii) A mutation in the *CG32397* gene (CG18769[c03230]) showed bristle defects similar to those of jv^1 and also failed to complement the jv^1 bristle phenotype, suggesting that jv^1 and CG18769[c03230] are two different alleles of the same gene. (iv) The transcript levels of *CG32397* are significantly reduced in *jv* mutants. (v) We found that expression of the CG32397 protein in bristles partially rescued *jv* bristle defects.

Since *CG32397* is a predicted gene, we analyzed its predicted transcript. Using PCR primer sets that cover the gene, along with 5′ RACE, we found that the first translation start site is actually located 165 bp downstream of the previously predicted start site.

As mentioned above, expression of the CG32397 protein rescues most *jv* bristle defects. There are several possible explanations for this partial rescue. (i) In the rescue experiments, we used actin-Gal4, which does not necessarily act as an endogenous *jv* promoter. (ii) It is possible that *CG32397* contains more alternative splice forms that we failed to detect in our molecular analysis. If this is indeed the case, it is possible that the other variants are needed for full rescue. (iii) Our rescue construct contained the entire open reading frame coding for the protein but lacked both the 5′ and 3′ ends. It is possible that these ends are required for the full function of the gene. Still, we believe that our results described above together with our finding that CG32397 is an actin-associated protein (see below) demonstrate that the *CG32397* gene encodes Jv.

Jv is an actin-associated protein. Bioinformatics analysis predicts that the *jv* gene encodes a protein that does not contain any known domain. To better understand the function of the protein, we expressed Jv, fused to GFP, in fly bristles and ovaries. We determined the localization of this GFP-fused protein in bristles and found that it colocalized to the actin bundles. These results reinforced our finding that *CG32397* encodes Jv, which is required for actin assembly during bristle development.

Next, we analyzed the effects of ectopically expressed Jv in other tissues. Accordingly, we used the *Drosophila* egg chamber as a model tissue. We found that expressing Jv in the germ line led to formation of an ectopic actin network that surrounds the nurse cell nucleus. Interestingly, examination of egg chambers at stage 14 revealed that in the nurse cells, Jv-GFP is also colocalized with actin that surrounds the nurse cell nucleus. This actin network is found in wild-type egg chambers and plays an important role in rapid cytoplasm transport from the nurse cell into the oocyte in a process termed dumping (10, 16). Thus, we suggest that expression of *CG32397* protein led to the premature formation of the actin network, surrounding the nurse cell nucleus, which is required at later stages of egg chamber development.

To conclude, the association of the Jv protein with the actin network, along with the effects of *jv* mutants on actin bundle formation in the bristle, suggests that Jv is a novel protein which functions in actin assembly.

ACKNOWLEDGMENTS

We thank Greg Guild, VDRC Austria, and the Bloomington Stock Center for generously providing fly strains and reagents.

This research was supported by Israel Science Foundation Grant 968/10 (to U.A.).

REFERENCES

1. **Abdu, U., D. Bar, and T. Schupbach.** 2006. Spn-F encodes a novel protein that affects oocyte patterning and bristle morphology in *Drosophila*. Development **133:**1477–1484.
2. **Bitan, A., G. M. Guild, D. Bar-Dubin, and U. Abdu.** 2010. Asymmetric microtubule function is an essential requirement for polarized organization of the *Drosophila* bristle. Mol. Cell. Biol. **30:**496–507.
3. **Brand, A. H., and N. Perrimon.** 1993. Targeted gene expression as a means of altering cell fates and generating dominant phenotypes. Development **118:**401–415.
4. **Cant, K., B. A. Knowles, M. S. Mooseker, and L. Cooley.** 1994. Drosophila singed, a fascin homolog, is required for actin bundle formation during oogenesis and bristle extension. J. Cell Biol. **125:**369–380.
5. **Fei, X., B. He, and P. N. Adler.** 2002. The growth of *Drosophila* bristles and laterals is not restricted to the tip or base. J. Cell Sci. **115:**3797–3806.
6. **Frank, D. J., R. Hopmann, M. Lenartowska, and K. G. Miller.** 2006. Capping protein and the Arp2/3 complex regulate nonbundle actin filament assembly to indirectly control actin bundle positioning during *Drosophila melanogaster* bristle development. Mol. Biol. Cell **17:**3930–3939.
7. **Grieshaber, S. S., D. H. Lankenau, T. Talbot, S. Holland, and N. S. Petersen.** 2001. Expression of the 53 kD forked protein rescues F-actin bundle formation and mutant bristle phenotypes in *Drosophila*. Cell Motil. Cytoskeleton **50:**198–206.
8. **Guild, G. M., P. S. Connelly, L. Ruggiero, K. A. Vranich, and L. G. Tilney.** 2003. Long continuous actin bundles in *Drosophila* bristles are constructed by overlapping short filaments. J. Cell Biol. **162:**1069–1077.
9. **Guild, G. M., P. S. Connelly, K. A. Vranich, M. K. Shaw, and L. G. Tilney.** 2002. Actin filament turnover removes bundles from *Drosophila* bristle cells. J. Cell Sci. **115:**641–653.
10. **Gutzeit, H. O.** 1986. The role of microfilaments in cytoplasmic streaming in Drosophila follicles. J. Cell Sci. **80:**59–169.
11. **Lees, A. D., and C. H. Waddington.** 1942. The development of the bristles in normal and some mutant types of *Drosophila melanogaster*. Proc. R. Soc. Lond. B Biol. Sci. **131:**87–110.
12. **Livak, K. J., and T. D. Schmittgen.** 2001. Analysis of relative gene expression data using real-time quantitative PCR and the $2^{-\Delta\Delta CT}$ method. Methods **25:**402–408.
13. **Mitchell, H. K., and L. S. Lipps.** 1978. Heat shock and phenocopy induction in Drosophila. Cell **15:**907–918.
14. **Morata, G., and P. Ripoll.** 1975. Minutes: mutants of *Drosophila* autonomously affecting cell division rate. Dev. Biol. **42:**211–221.
15. **Negeri, D., H. Eggert, R. Gienapp, and H. Saumweber.** 2002. Inducible RNA interference uncovers the Drosophila protein Bx42 as an essential nuclear cofactor involved in Notch signal transduction. Mech. Dev. **117:**151–162.
16. **Ogienko, A. A., S. A. Fedorova, and E. M. Baricheva.** 2007. Basic aspects of ovarian development in *Drosophila melanogaster*. Genetika **43:**1341–1357.
17. **Otani, T., et al.** 2011. IKKε regulates cell elongation through recycling endosome shuttling. Dev. Cell **20:**219–232.
18. **Spradling, A. C., and G. M. Rubin.** 1982. Transposition of cloned P elements into *Drosophila* germ line chromosomes. Science **218:**341–347.
19. **Tilney, L. G., M. S. Tilney, and G. M. Guild.** 1995. F-actin bundles in *Drosophila* bristles. I. Two filament cross-links are involved in bundling. J. Cell Biol. **130:**629–638.
20. **Tilney, L. G., P. Connelly, S. Smith, and G. M. Guild.** 1996. F-actin bundles in *Drosophila* bristles are assembled from modules composed of short filaments. J. Cell Biol. **135:**1291–1308.

21. **Tilney, L. G., P. S. Connelly, K. A. Vranich, M. K. Shaw, and G. M. Guild.** 1998. Why are two different cross-linkers necessary for actin bundle formation in vivo and what does each cross-link contribute? J. Cell Biol. **143:**121–133.
22. **Tilney, L. G., P. S. Connelly, K. A. Vranich, M. K. Shaw, and G. M. Guild.** 2000. Actin filaments and microtubules play different roles during bristle elongation in Drosophila. J. Cell Sci. **113:**1255–1265.
23. **Tilney, L. G., P. S. Connelly, K. A. Vranich, M. K. Shaw, and G. M. Guild.** 2000. Regulation of actin filament cross-linking and bundle shape in *Drosophila* bristles. J. Cell Biol. **148:**87–99.
24. **Tilney, L. G., et al.** 2004. The role actin filaments play in providing the characteristic curved form of *Drosophila* bristles. Mol. Biol. Cell **15:**5481–5491.